

# Catalysis Science & Technology

Accepted Manuscript



This is an *Accepted Manuscript*, which has been through the Royal Society of Chemistry peer review process and has been accepted for publication.

*Accepted Manuscripts* are published online shortly after acceptance, before technical editing, formatting and proof reading. Using this free service, authors can make their results available to the community, in citable form, before we publish the edited article. We will replace this *Accepted Manuscript* with the edited and formatted *Advance Article* as soon as it is available.

You can find more information about *Accepted Manuscripts* in the [Information for Authors](#).

Please note that technical editing may introduce minor changes to the text and/or graphics, which may alter content. The journal's standard [Terms & Conditions](#) and the [Ethical guidelines](#) still apply. In no event shall the Royal Society of Chemistry be held responsible for any errors or omissions in this *Accepted Manuscript* or any consequences arising from the use of any information it contains.

## PAPER

# A mild route to solid-supported rhodium nanoparticle catalysts and their application to the selective hydrogenation reaction of substituted arenes<sup>†</sup>

Cite this: DOI: 10.1039/x0xx00000x

Received 00th January 2012,  
Accepted 00th January 2012

DOI: 10.1039/x0xx00000x

www.rsc.org/catalysis

Carmen Moreno-Marrodan,<sup>a</sup> Francesca Liguori,<sup>a</sup> Elisabet Mercadé,<sup>b</sup> Cyril Godard,<sup>b</sup> Carmen Claver<sup>b</sup> and Pierluigi Barbaro<sup>\*a</sup>

A clean route is described for the preparation of 1.3 % (w/w) supported rhodium nanoparticle ( $3.0 \pm 0.7$  nm) catalysts onto commercial ion-exchange resins. Their application to the liquid-phase hydrogenation reaction of C=C bonds shows the most active species are obtained under catalytic conditions at room temperature and 1 bar H<sub>2</sub>. The heterogeneous catalyst shows excellent activity, selectivity and reusability in the hydrogenation reaction of alkenes and substituted arenes under very undemanding conditions. The results are discussed in terms of support effect on the catalytic efficiency.

## Introduction

Rhodium nanoparticles (RhNP), either colloidal dispersions or solid-supported, are pivotal in catalysis because of the unique performance provided in several oxidation, carbonylation, coupling and hydrogenation reactions, compared to other transition metals.<sup>1</sup> Particularly, the (stereo)selective hydrogenation reaction of substituted, monocyclic arenes to cyclohexane derivatives is a reaction of much practical interest in the polymer, fuel and fine-chemicals sector, that is usually achieved under mild and more drastic conditions using homogeneous and heterogeneous Rh catalysts, respectively.<sup>2</sup> However, the preference of the chemical industry for solid catalysts due to environmental and economic constraints,<sup>3,4</sup> combined with the cost and rarity of rhodium,<sup>5,6</sup> pushes chemists to devise innovative protocols for heterogeneous RhNP catalysts which comply with sustainability criteria. The task is challenging since solid-supported metal nanoparticles (MNP) are usually affected by multiple drawbacks, which include: i) synthetic procedures requiring toxic reagents, harsh

conditions or sophisticated equipments, ii) lack of control over MNP size and distribution, iii) lack of reproducibility, iv) lack of stability under reaction conditions, v) applicability only to specific reaction-support combinations.<sup>7,8</sup>

Compared to other insoluble support materials, ion-exchange resins offer a number of advantages for the production of MNP-based catalysts:<sup>9,10</sup>

- low cost,
- commercial availability in various chemical and physical modifications,
- satisfactory chemical, mechanical and thermal resistance,
- ease of handling,
- straightforward, non-covalent metal anchoring,
- MNP stabilization by the dual effect of charged functional groups (electrostatic stabilization),<sup>11</sup> and porosity (steric stabilization),<sup>12</sup>
- facile integration in existing reactor equipments,
- versatility in terms of accessible reactions.

In particular, low-cross linked resins (0.5-4%) develop a microporous gel structure when swollen in an appropriate solvent, allowing for the accommodation of narrow size distributions of MNP.<sup>13</sup> Despite of these favourable features, ion-exchange resin-supported RhNP catalysts are almost unexplored, most applications focussing on palladium, platinum and gold particles.<sup>14,15</sup>

Based on the green strategy we have developed for the immobilization of PdNP onto ion-exchange resins,<sup>16,17</sup> herein we report on the synthesis and characterisation of resin-

<sup>a</sup> Consiglio Nazionale delle Ricerche, Istituto di Chimica dei Composti Organo Metallici, Via Madonna del Piano 10, 50019 Sesto Fiorentino, Firenze, Italy. E-mail: pierluigi.barbaro@iccom.cnr.it

<sup>b</sup> Department of Physical and Inorganic Chemistry, Universitat Rovira I Virgili, C/Marcel·lí Domingo s/n, Campus Sescelades, 43007, Tarragona, Spain.

<sup>†</sup> Electronic Supplementary Information (ESI) available: catalytic experiment results table. See DOI: 10.1039/b000000x/

supported RhNP, and their use in the heterogeneous, liquid-phase catalytic hydrogenation reaction of substituted arenes.

## Experimental

### General information

Unless otherwise stated, all manipulations were performed under nitrogen atmosphere by using standard Schlenk techniques. DOWEX® 50WX2-100 (H<sup>+</sup> form, 2% cross-linked, gel-type, 50-100 mesh [150-300 µm] bead size, 4.8 meq/g exchange capacity), DOWEX® 50WX2-400® strong cation-exchange resins (H<sup>+</sup> form, 2% cross-linked, gel-type, 200-400 mesh [38-75 µm] bead size, 4.8 meq/g exchange capacity) were obtained from Aldrich. The commercial resins were treated as follows prior of use to remove incidental impurities. 20 g of resin were washed with refluxing deionised water for 2 h and with refluxing methanol for 1 h using a Soxhlet apparatus in air. After cooling to room temperature, the resin was washed with dichloromethane (3 x 100 mL), methanol (3 x 100 mL) and diethyl ether (3 x 100 mL). The resin was dried under a stream of nitrogen and stored under nitrogen. The lithiated resin was prepared by adding 5 g of the purified protonated resin to a 1 M solution of lithium hydroxide (150 mL) in air atmosphere. The mixture was stirred at 150 rpm at room temperature for 24 h using an orbital stirrer. The resin obtained was placed in a glass filter and washed repeatedly with deionised water (5 x 100 mL) until neutral pH of the washings. Then, it was washed with methanol (3 x 100 mL) and diethyl ether (3 x 100 mL) and dried in a stream of nitrogen. The product obtained as white beads was stored under nitrogen. [Rh(NBD)<sub>2</sub>]BF<sub>4</sub> was obtained from Alfa Aesar and used as received (NBD = bicyclo[2.2.1]hepta-2,5-diene). All other reagents were commercial products and were used as received without further purifications.

ESEM (Environmental Scanning Electron Microscopy) measurements were performed on a FEI Quanta 200 microscope operating at 25 KeV accelerating voltage in the low-vacuum mode (1 torr) and equipped with an EDAX Energy Dispersive X-ray Spectrometer (EDS). X-ray maps were acquired on the same instrument using a 512x400 matrix, 25 KeV accelerating voltage and 350 µm horizontal full width. TEM (Transmission Electron Microscopy) measurements were carried out using a CM12 PHILIPS instrument. The sample preparation was carried out by dispersing the grinded resin into 1 mL of ethanol and treating the solution in an ultrasonic bath for 30 min. A drop of solution was deposited onto a carbon coated Cu TEM grid and the solvent left to evaporate. Statistical nanoparticle size distribution analysis was typically carried out on 300-400 particles. XRD (X-ray Diffraction) spectra were recorded with a PANalytical XPERT PRO powder diffractometer, employing CuKα radiation ( $\lambda = 1.54187 \text{ \AA}$ ), a parabolic MPD-mirror and a solid state detector (PIXcel). Reactions under batch conditions were performed using a stainless steel autoclave constructed at ICCOM-CNR (Firenze, Italy) and equipped with a magnetic stirrer, a Teflon® inset and a pressure controller for higher pressures. GC

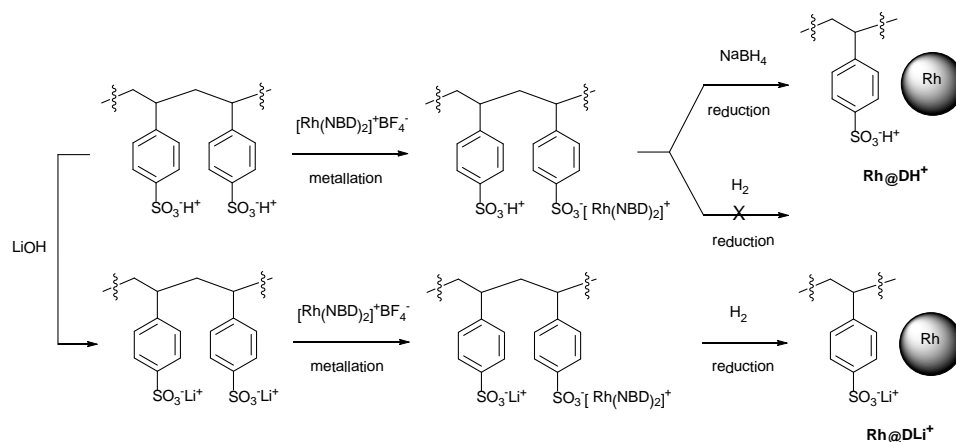
analyses were performed on a Shimadzu GC-2010 gas chromatograph equipped with a flame ionization detector and either a Varian VF-WAXms (30 m, 0.25 mm ID, 0.25 µm FT) or a Supelco SPB-1 (30 m, 0.25 mm ID, 0.25 µm FT) capillary column. GC-Ms analyses were performed on a Shimadzu QP2010S spectrometer equipped with identical capillary columns. The metal content in the resin-supported catalysts was determined by Atomic absorption spectrometry (AAS) using a AANALYST200 spectrometer. Each sample (50-100 mg) was treated in a microwave-heated digestion bomb (Milestone, MLS-200, 20 min. @ 220 °C) with concentrated HNO<sub>3</sub> (1.5 mL), 98% H<sub>2</sub>SO<sub>4</sub> (2 mL), and 0.5 mL of H<sub>2</sub>O<sub>2</sub> 30%. The content of metal leached in the solutions recovered after catalysis was determined by Inductively Coupled Plasma Atomic Emission Spectroscopy (ICP-OES) with a Varian 720ES instrument at a sensitivity of 500 ppb. The detection limit for Rh was 0.01 ppm. The solutions were analysed directly after 1:5 dilution in 0.1 M hydrochloric acid.

### Preparation of resin-supported rhodium(I) species

In a typical procedure, 1 g of dry cation-exchange resin, either lithiated or protonated form, was swollen in 30 mL of degassed methanol followed by the addition of a degassed solution of bis(norbornadiene) rhodium(I) tetrafluoroborate (54.4 mg, 0.145 mmol, ratio Rh/sulfonic groups = 1/33) in methanol (26 mL). The mixture was stirred under nitrogen atmosphere and room temperature for 2 h using an orbital stirrer. The resin obtained was transferred into a glass filter via a Teflon tube under nitrogen and washed sequentially with methanol (3 x 75 mL) and diethyl ether (3 x 75 mL), before being dried in a stream of nitrogen overnight. The rhodium containing resin obtained as yellow beads was stored under nitrogen in the dark. AAS analysis showed the resin to contain 1.3 % (w/w) of Rh, corresponding to a 87% metal uptake.

### Preparation of resin-supported rhodium(0) species

Method a) Reduction with NaBH<sub>4</sub>: solid NaBH<sub>4</sub> (82.5 mg, 2.18 mmol) was slowly added to 0.5 g of 1.3% (w/w) rhodium(I)-resin in 28 mL of methanol. The resin became immediately black. The suspension was stirred at 200 rpm at room temperature for 2h, using an orbital stirrer. The resin obtained was transferred into a glass filter via a Teflon tube under nitrogen and washed with methanol (3 x 75 mL) and diethyl ether (3 x 75 mL), and then dried in a stream of nitrogen overnight. The product, obtained as black beads, was stored under nitrogen in the dark. Method b) Reduction with a flow of H<sub>2</sub>: 0.5 g of 1.3% (w/w) rhodium(I)-resin were suspended in 28 mL of methanol under nitrogen. Hydrogen gas was bubbled at 1 bar at room temperature for 2 h under orbital stirring at 170 rpm. The resin became slowly black (*ca.* 10 min.). After that time, the resin was transferred into a glass filter under nitrogen via a Teflon tube, it was washed with methanol (3 x 75 mL), diethyl ether (3 x 75 mL) and then dried in a stream of nitrogen overnight. The product, obtained as black beads, was stored under nitrogen in the dark. Method c) Reduction with a flow of H<sub>2</sub> in the presence of an excess of substrate (catalytic conditions):



**Scheme 1** Sketch of ion-exchange resins-supported RhNP synthesis with labelling scheme adopted.

0.05 g of 1.3% (w/w) rhodium(I)-resin were swollen in 5 mL of methanol under nitrogen. A substrate solution in methanol was then added and the mixture heated and pressurized with H<sub>2</sub> gas at the desired temperature and pressure. After completion of the catalytic reaction, the resin was transferred into a glass filter under nitrogen via a Teflon tube, washed with methanol (3 x 75 mL), diethyl ether (3 x 75 mL) and then dried in a stream of nitrogen overnight. The product, obtained as black beads, was stored under nitrogen in the dark.

Irrespective of the reduction method, AAS analysis showed the Rh content in the resin was unchanged 1.3% (w/w).

### Hydrogenation reactions and catalyst recycle

In a typical experiment, the resin-supported Rh species, either Rhodium(0) or Rhodium(I) (50 mg, *ca.* 1.3% Rh w/w, *ca.* 0.006 mmol of rhodium), was swollen in 5 mL of degassed methanol. After 5 minutes a solution of the substrate (1.45 mmol) in methanol (4.1 mL) was added under nitrogen. Hydrogen gas was then bubbled at 1 bar H<sub>2</sub> and 10 mL/min at room temperature, under stirring at 170 rpm with an orbital stirrer. The H<sub>2</sub> inlet was taken as the start time of the reaction. After the desired time, the methanol solution was completely removed under a stream of hydrogen using a gas-tight syringe. A sample of this solution (0.5 µL) was used for GC and GC-MS analysis, while the remaining aliquot was used for the catalyst leaching test and ICP-OES measurement. A fresh solution of the substrate (1.45 mmol) in methanol (9.1 mL) was then transferred under hydrogen into the flask containing the recovered supported species. The mixture was stirred at 170 rpm and room temperature under hydrogen flow and, after the desired time, the mixture was treated as described above. The same recycling procedure was used in the subsequent hydrogenation cycles. After use in catalysis, the solid species was washed with methanol (3 x 10 mL) and diethyl ether (3 x 10 mL), dried in a stream of nitrogen overnight and stored under nitrogen for later characterization. The reaction products were identified by GC retention times and GC-MS analysis. For

reactions carried out at higher temperatures and/or pressures, the supported Rh species (50 mg, *ca.* 1.3% Rh w/w, *ca.* 0.006 mmol of rhodium) was placed in a metal free autoclave that was immediately closed and degassed with 3 cycles vacuum/nitrogen. A solution of the substrate (1.45 mmol) in methanol (9.1 mL) was then transferred under nitrogen into the reactor using a cannula and nitrogen was replaced by hydrogen with 3 cycles pressurization/depressurization. After setting up the desired temperature and pressure, the solution was magnetically stirred at 170 rpm.

## Results and discussion

### Catalyst synthesis and characterization

We have recently reported a friendly method for the growth of PdNP within the pores of gel-type ion-exchange resins.<sup>16</sup> In the present work, we have extended the methodology to the synthesis of RhNP. The approach involves metallation of the resin by ion-exchange using an appropriate metal precursor, *i.e.* a soluble cationic specie whose metal centre can be smoothly reduced,<sup>18</sup> followed by reduction under 1 bar H<sub>2</sub> and room temperature. A schematic representation of the two-step procedure is reported in Scheme 1. The resins used were the commercial, strong cation-exchange sulfonic gels DOWEX® (2% cross-linkage), either 50-100 mesh (150-300 µm) or 200-400 mesh (38-75 µm) bead size. The polymers were employed in their protonated form as manufactured, or converted into the corresponding lithium salt.<sup>19</sup> [Rh(NBD)<sub>2</sub>]BF<sub>4</sub> was selected as metal precursor due to its solubility in methanol, required for optimal resin swelling, and to the known propensity to H<sub>2</sub> metal reduction *via* norbornene elimination.<sup>20</sup> Indeed, first step metallation in methanol using a 33 : 1 = meq exchange capacity : mmol Rh ratio afforded a yellow material, whose treatment with H<sub>2</sub> under very mild conditions (rt, 1 bar H<sub>2</sub>, *ca.* 10 min.) gave rhodium(0)-containing black beads featuring a typical 1.3% bulk Rh loading (w/w, ICP-OES), which corresponds to a metal uptake of *ca.* 87%. Importantly, the H<sub>2</sub> reduction was

**Table 1** Resin-supported RhNP catalysts prepared

Label	Resin <sup>a</sup>		Reduction method	Rh <sup>c</sup> (%)
	Ionic form	Size (μm) <sup>b</sup>		
Rh@D100H <sup>+</sup>	H <sup>+</sup>	150-300	NaBH <sub>4</sub>	1.3(1)
Rh@D400H <sup>+</sup>	H <sup>+</sup>	38-75	NaBH <sub>4</sub>	1.3(1)
Rh@D100Li <sup>+</sup>	Li <sup>+</sup>	150-300	H <sub>2</sub> (rt, 1 bar H <sub>2</sub> )	1.3(1)
Rh@D400Li <sup>+</sup>	Li <sup>+</sup>	38-75	H <sub>2</sub> (rt, 1 bar H <sub>2</sub> )	1.3(1)
Rh@D400Li <sup>+</sup> <i>in situ</i>	Li <sup>+</sup>	38-75	H <sub>2</sub> , <i>in situ</i> <sup>d</sup>	1.3(1)

<sup>a</sup> DOWEX 50WX2, 100 or 400 mesh. <sup>b</sup> Bead diameter. <sup>c</sup> Rh loading (w/w) from ICP-OES. <sup>d</sup> Under the conditions of catalytic reaction. 0.16 M substrate solution in CH<sub>3</sub>OH, substrate / Rh molar ratio = 230.

successful only in the case of the lithiated resins, since *use of NaBH<sub>4</sub> was required to achieve metal reduction on the protonated polymers*. This finding can be attributed to the different reduction potentials of rhodium in acidic medium.<sup>21</sup> Further, in order to directly use the metallated resins in catalysis without a pre-reduction step (*vide infra*), and to ascertain the effect of the preparation method on the catalyst activity, as previously explored for PdNP,<sup>16</sup> the synthesis of RhNP was also accomplished *in-situ* by carrying out the reduction of rhodium(I)-supported species *under catalytic hydrogenation conditions, i.e. in the presence of H<sub>2</sub> and an excess of substrate in methanol*. Catalyst characterization was performed at the end of the catalytic reaction, in that case. A summary of the catalysts prepared is reported in Table 1.

Previously reported methods for solid-supported RhNP synthesis involve impregnation-reduction methods using RhCl<sub>3</sub> or Rh(NH<sub>3</sub>)<sub>6</sub>Cl<sub>3</sub> and sodium borohydride (montmorillonite,<sup>22</sup> silica,<sup>23</sup> CNT<sup>24</sup>), Rh(CH<sub>3</sub>CO<sub>2</sub>)<sub>2</sub>, Rh(NO<sub>3</sub>)<sub>3</sub> or RhCl<sub>3</sub> followed by calcination and high-temperature H<sub>2</sub> reduction (873 K alumina,<sup>25</sup> 973 K ceria,<sup>26</sup> 1273 K zirconia<sup>27</sup>, 1123 K MgAl<sub>2</sub>O<sub>4</sub>,<sup>28</sup> 673 K silica<sup>29</sup>). Other methods include heterogenization of preformed RhNP (silica,<sup>30</sup> zirconia,<sup>31</sup> alumina,<sup>32</sup> titania<sup>33</sup>), vapour deposition (silica<sup>34</sup>), flame spray pyrolysis (alumina<sup>35</sup>) and laser ablation (silica<sup>36</sup>) techniques.<sup>37</sup> It is worth mentioning that RhNP onto magnesium oxide have been recently obtained by deposition-reduction of [Rh(COD)(μ-OCH<sub>3</sub>)<sub>2</sub>]<sub>2</sub> by H<sub>2</sub> under slightly heavier conditions than those herein reported (50 °C, 3.4 bar).<sup>38</sup>

In the present study, all Rh-containing resins were characterized in the solid state by a combination of microscopic and scattering techniques.

ESEM experiments showed that the resin beads are not damaged by metallation, reduction or use in catalysis, as no signs of breakage or cracking were detected anyhow. EDS maps recorded on sections of rhodium(I) contained beads showed a homogeneous metal distribution within the solid support, in both the protonated and lithiated resins, indicating that the solvent diffuses thoroughly into and out the bead during the metallation step.<sup>19</sup> On the contrary, maps of pre-reduced supported rhodium(0) species revealed egg-shell and uniform

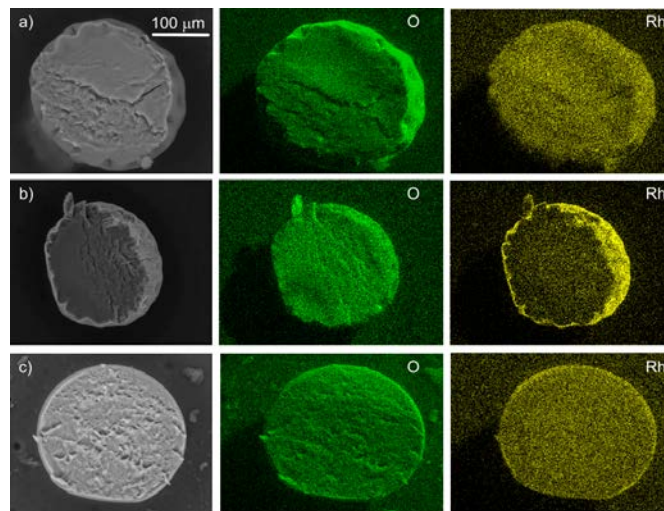


**Fig. 1** ESEM images (left, backscattered electrons) and EDS X-ray maps of oxygen (center, O Kα1) and rhodium (right, Rh La1) of: (a) rhodium(I)@D100Li<sup>+</sup> bead section before reduction (b) Rh@D100Li<sup>+</sup> after Rh reduction, (c) Rh@D100H<sup>+</sup> after Rh reduction (25 KeV, 650 magnifications).

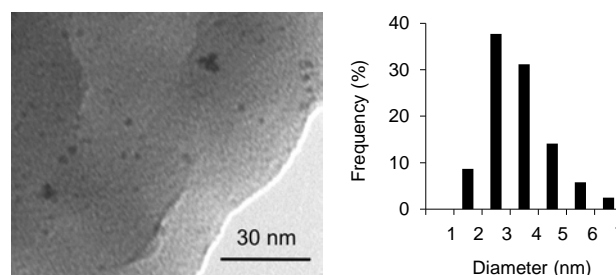
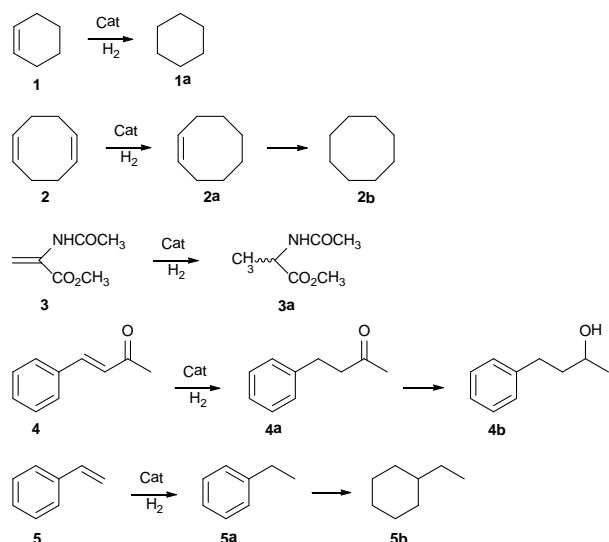


**Fig. 2** Representative TEM image (left) and RhNP size distribution (right) of Rh@D400H<sup>+</sup>.

metal distributions in the case of Rh@DLi<sup>+</sup> (H<sub>2</sub> reduction) and Rh@DH<sup>+</sup> (NaBH<sub>4</sub> reduction), respectively. This is clearly visible from the backscattered electron images and from the oxygen and Rh maps, reported for comparison in Fig. 1, before and after rhodium reduction.<sup>39</sup> A similar finding was previously observed for other resin-supported MNP species (M = Pd, Ru, Au)<sup>40</sup> and was ascribed to difference in the rate of metal cation diffusion within the solid matrix, as a consequence of the concentration gradient generated by its reduction, and the rate of diffusion of the reducing agent.<sup>41</sup> Egg-shell distributions may be observed in the instance that the diffusion of the cation is faster than that of the reductant.

Irrespective of synthetic method or the resin type, XRD and TEM analyses showed the presence of agglomerates up to 30 nm diameter consisting of embedded single RhNP having a mean size of 3.0 ± 0.7 nm. Fig. 2 reports a typical TEM image and the corresponding RhNP size distribution in Rh@DH<sup>+</sup> species. The RhNP size calculated from the characteristic reflexion of the [111] crystallographic plane (2θ = 41°) in the XRD pattern was 3.1 nm (Fig. S1), in complete agreement with the TEM values of single particles. RhNP agglomeration was



**Scheme 2** Sketch of probe substrates examined and products detected with labelling scheme

**Table 2** Catalytic hydrogenation reaction using Rh@D100H<sup>+</sup> under 1 bar H<sub>2</sub> pressure and room temperature <sup>a</sup>

Entry	Substrate	Conversion (%)	TOF <sup>b</sup> (h <sup>-1</sup> )	Product	Selectivity <sup>c</sup> (%)
1	<b>1</b>	98.1	838.9	<b>1a</b>	98.7 <sup>d</sup>
2	<b>2</b>	91.0	259.3	<b>2a</b>	63.8
3	<b>3</b>	99.8	56.9 <sup>e</sup>	<b>3a</b>	100.0
4	<b>4</b>	93.7	82.1	<b>4a</b>	92.4
5	<b>5</b>	94.9	270.4	<b>5a</b>	100.0

<sup>a</sup> Reaction conditions: methanol, substrate : Rh = 570 : 1 molar ratio, 50 mg catalyst 1.3 % (w/w) Rh. Data from GC analysis. <sup>b</sup> Turnover frequency, as: (mol substrate converted) / (mol Rh × h) calculated at the conversion indicated and on bulk Rh content. <sup>c</sup> For example, **2a** selectivity = **2a**/(**2a**+**2b**). <sup>d</sup> Benzene ca. 1%. <sup>e</sup> Substrate / Rh ratio = 114.

already described for other solid-supported systems, that was suggested to take place during the formation of metallic rhodium.<sup>22b,38</sup> No major changes were observed in TEM and XRD data for Rh@D after use in catalysis, which indicates the sinter-stability of the resin-supported particles. Chemisorption studies were hampered by the limited accessibility of gas reactants to gel-type resin-embedded metal NP.<sup>42,43</sup>

### Catalytic hydrogenation reactions

The resin-supported RhNP were tested as catalysts in hydrogenation reactions under batch conditions, either as pre-reduced species or prepared *in-situ*. In the latter case, the rhodium(I)-metallated resins were directly added to the substrate solution under nitrogen, before the mixture was exposed to the desired H<sub>2</sub> pressure and temperature, which was taken as the start time of the catalytic reaction. All supported catalysts showed to be effective under very undemanding

conditions in methanol solutions, albeit with remarkable differences depending on various factors affecting their performance. To ascertain the catalysts versatility, a number of probe substrates bearing different functionalities were scrutinized.

### CATALYST ACTIVITY, SELECTIVITY AND REUSABILITY

In order to get a first evaluation of the efficiency of the catalysts family, the hydrogenation of simple substrates subject to minor selectivity issues, i.e. cyclohexene (**1**), 1,5-cyclooctadiene (**2**), methyl-2-acetamidoacrylate (**3**), *trans*-4-phenyl-3-buten-2-one (**4**) and styrene (**5**) was carried out using Rh@D100H<sup>+</sup> species under 1 bar H<sub>2</sub> and room temperature. A sketch of the substrates investigated and the reaction products detected is reported in Scheme 2. Irrespective of the substrate, the catalyst showed to be quite active under the above reaction conditions affording nearly quantitative conversions within reasonable timeframes. Representative data are reported in Table 2 in terms of conversion, selectivity and turnover frequency (TOF) based on bulk rhodium content.

The hydrogenation of **1** to cyclohexane **1a** was achieved with a productivity of 838.9 h<sup>-1</sup>, that likens to that previously reported for the parent resin-supported Rh@MonoBor system under comparable flow conditions (rt, 1.8 bar H<sub>2</sub>, 1020 h<sup>-1</sup>).<sup>44</sup> The analogous Pd@D100 catalyst was less active under the same reaction conditions (TOF = 414 h<sup>-1</sup>).<sup>45</sup> The solvent-free hydrogenation of cyclohexene by solid-supported RhNP was recently described with hydroxyapatite (rt, 1 bar H<sub>2</sub>, TOF = 10 h<sup>-1</sup>)<sup>46</sup>, silica-coated magnetite nanoparticles (25 °C, 1 bar H<sub>2</sub>, TOF = 2638 h<sup>-1</sup>)<sup>47</sup> and 5% Rh@MgO (25 °C, 5 bar H<sub>2</sub>, TOF = 15667 h<sup>-1</sup> calculated on exposed Rh).<sup>38</sup>

The hydrogenation of **2** gave 63.8% of the partial hydrogenation product cyclooctene **2a** at 91.0% conversion, which is less efficient than the corresponding Pd catalyst (96.7% sel. at 98.5% conv., TOF = 418 h<sup>-1</sup>).<sup>45</sup>

Chemoselectivity of C=C *versus* C=O hydrogenation was tested with **4** resulting in 92% selectivity to 4-phenyl-butan-2-one (**4a**) at 94% conversion, with formation of **4b** and traces of ketals by-products. Best results for the partial hydrogenation of **4** were previously obtained using the resin-supported Pd@MonoBor catalyst under continuous flow (rt, 1.5 bar H<sub>2</sub>, 96.0% sel. at 99.5% conv., TOF = 166 h<sup>-1</sup>),<sup>44</sup> and Pd@SiO<sub>2</sub> in batch (70 °C, 1 bar H<sub>2</sub>, 99.0% sel. at 100% conv.).<sup>48</sup>

The hydrogenation of **5** gave ethylbenzene **5a** with good productivity (TOF = 270.4 h<sup>-1</sup>), with no traces of ethylcyclohexane **5b** detected under these conditions.

The supported catalyst could be quantitatively recovered by decantation and reused by addition of identical amounts of substrate solution under hydrogen. Recycling experiments showed negligible activity decay upon recycle over five consecutive runs under the same reaction conditions. Representative results are reported in graphical format in Fig. 3 for **2** and **5**. Rh leaching in solution was negligible in each run (ICP-OES), while the absence of catalytic activity of the recovered reaction solutions indicated the catalyst to be truly heterogeneous, ruling out the contribution of homogeneous

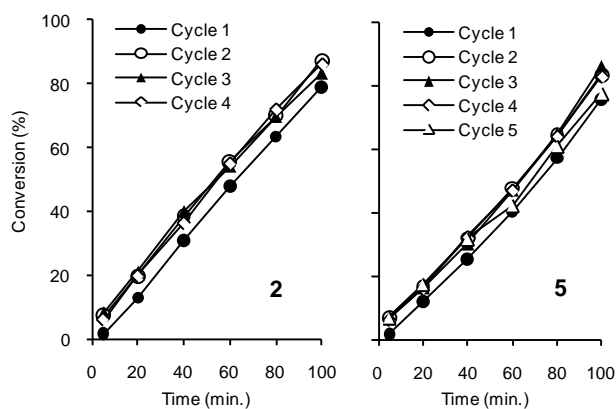


**Fig. 3** Reuse of Rh@D100H<sup>+</sup> catalyst in the hydrogenation reaction of **2** (left) and **5** (right). Reaction conditions: substrate 1.03 M in CH<sub>3</sub>OH, 50 mg catalyst 1.3 % (w/w) Rh, substrate / catalyst molar ratio 570, rt, 1 bar H<sub>2</sub>. Data from GC analysis.

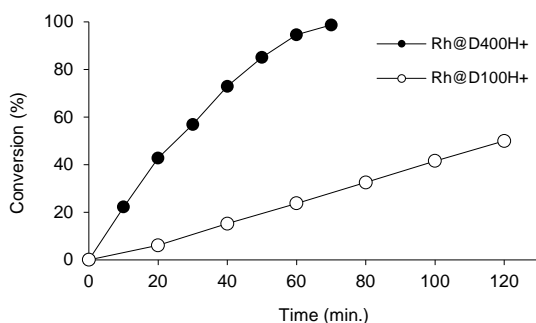


**Fig. 4** Hydrogenation reaction of **3** using catalysts with different bead size. Reaction conditions: substrate 0.16 M in CH<sub>3</sub>OH, 50 mg catalyst 1.3 % (w/w) Rh, substrate / catalyst molar ratio 290, rt, H<sub>2</sub> 1 bar. Data from GC analysis.

species to the catalytic conversion.<sup>49</sup> No significant changes in catalyst selectivity was observed upon reuse. The above findings are in line with those previously reported for the parent resin-supported PdNP hydrogenation catalysts,<sup>16</sup> and indicate the strong metal anchoring on the support under the conditions of catalysis.<sup>50</sup>

#### EFFECT OF THE PARTICLE SIZE

Since it is known that gel-type ion-exchange resins are affected by internal mass-transfer limitations,<sup>51</sup> we compared the activity of the catalysts supported onto resins of different bead size under the same experimental conditions.<sup>52,53</sup> Indeed, use of 38-75 μm beads, instead of 150-300 μm, invariably resulted in higher productivity, thus confirming that the kinetic of the hydrogenation reaction is ruled by the diffusion of the reagents inside the support. The finding is shown in Fig. 4 in which the hydrogenation data of **3** using Rh@D100H<sup>+</sup> and Rh@D400H<sup>+</sup> catalysts are reported. Despite of this, resins of larger size were preferably used in recycling experiments, due to their easier separation.

#### EFFECT OF THE PREPARATION METHOD

The performance of supported catalysts of the same bead-size, but prepared with different methods, was compared under

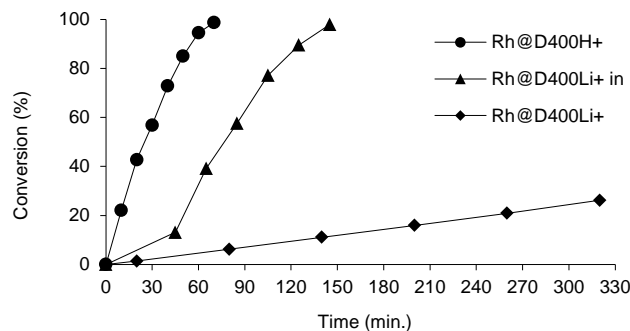


**Fig. 5** Hydrogenation reaction of **3** using Rh@D400 catalysts. Reaction conditions: substrate 0.16 M in CH<sub>3</sub>OH, 50 mg catalyst 1.3 % (w/w) Rh, substrate / catalyst molar ratio 290, rt, H<sub>2</sub> 1 bar. Data from GC analysis.

identical reaction conditions (rt, 1 bar H<sub>2</sub>, substrate:metal = molar ratio 290:1). *Regardless the substrate*, two major outcomes were apparent. First, the pre-reduced catalysts obtained by NaBH<sub>4</sub> reduction were more active than those obtained by H<sub>2</sub> pre-treatment. Data for the hydrogenation reaction of **3** using Rh@D400 catalysts are reported in graphical format in Fig. 5, as representative example. Thus, Rh@D400H<sup>+</sup> gave a 94.5% conversion after 1 h, whereas Rh@D400Li<sup>+</sup> resulted in 5% conversion after the same reaction time. An explanation for this result is not straightforward. A proton-acceleration effect by resin acid sites has been invoked for some metal-reaction combinations (Pd-hydroxylation,<sup>15b,54</sup> Ru-hydrogenation<sup>55</sup>), but not for others (Pd-hydrogenation<sup>16</sup>). On the other hand, lithiated resin supports usually show a higher efficiency compared to protonated ones, that was attributed to the better swelling due the higher solvation of lithium.<sup>19,56</sup> In the case in our hands, the different metal distributions within the beads (egg-shell or homogeneous) generated by the different preparation method may have consequences on their performance, although difficultly rationalizable. Small differences in the size of supported RhNP may also play a role, even if the lack of direct connection between size of RhNP and their catalytic activity was demonstrated.<sup>1c</sup>

Second, most importantly, *the activity of the catalysts prepared in-situ under catalytic conditions was invariably higher than that of the corresponding pre-reduced species*. In the case of Rh@D400 catalysts, the hydrogenation reaction of **3** was completed within 150 min. using the *in-situ* prepared Rh@D400Li<sup>+</sup> catalysts, whereas the conversion was as low as 12% using the pre-reduced specie Rh@D400Li<sup>+</sup> (Fig. 5).<sup>57</sup> An analogous behaviour was previously observed for the parent PdNP supported catalysts, which was attributed to an “excess of substrate stabilizing effect” responsible both for the limited growth of Pd nanoparticles under *in-situ* conditions, and for the stabilization of metastable Pd species, whose reactivity is higher than that of conventional Pd<sup>0,16,45</sup>. Inspection of Fig. 5 shows a short induction period (ca. 30 min. in the case in our hand), that can be safely ascribed to the time required to reduce the supported rhodium(I) to Rh<sup>0</sup>, followed by the generation of the specie featured by the highest catalytic activity.<sup>58</sup> Table 3

**Table 3** Hydrogenation reaction of **3** by ion-exchange resin-supported MNP catalysts <sup>a</sup>

Entry	Catalyst	Conversion (%)	Time <sup>b</sup> (min)	TOF <sup>c</sup> (h <sup>-1</sup> )	Ref.
1	Rh@D400H <sup>+</sup>	42.8	20	369	this work
2	Rh@D400Li <sup>+</sup> <i>in</i>	5.8	20	50	this work
3	Rh@D400Li <sup>+</sup>	1.4	20	12	this work
4	Rh@D100H <sup>+</sup>	6.0	20	41	this work
5 <sup>d</sup>	Pd@D100Li <sup>+</sup> <i>in</i>	100	20	750	45
6 <sup>d</sup>	Pd@D100Li <sup>+</sup>	97.0	20	727	45

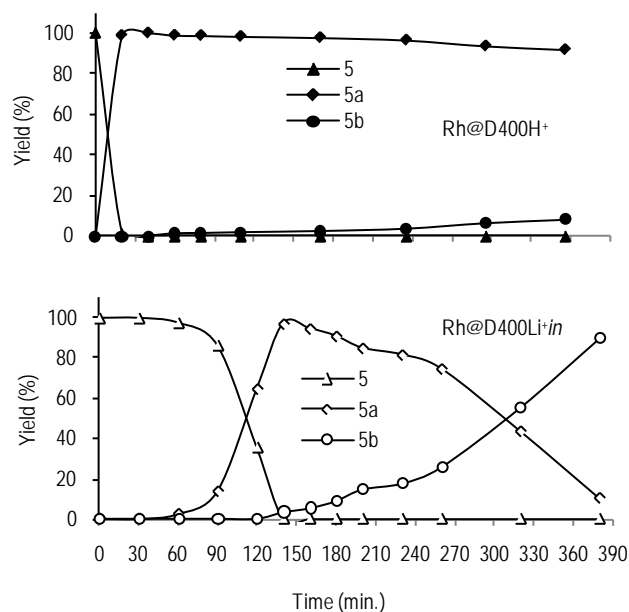
<sup>a</sup> Reaction conditions: methanol, 1 bar H<sub>2</sub> pressure, room temperature substrate : metal = 290 : 1 molar ratio, 50 mg catalyst, 1.3% (w/w) Rh, 1.25% (w/w) Pd. Data from GC analysis. <sup>b</sup> Reaction time. <sup>c</sup> Turnover frequency, as: (mol substrate converted) / (mol metal × h) calculated at the reaction time indicated and on bulk metal content. <sup>d</sup> Substrate : metal = 250 : 1 molar ratio.

summarizes the efficiency values reported in the literature for the hydrogenation reaction of **3** by resin-supported Rh and Pd catalysts under the same experimental conditions. TOF values are calculated at the same reaction time for comparative purposes.

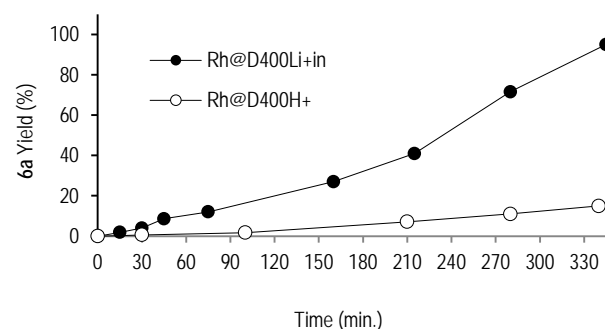
#### CATALYST SCOPE: HYDROGENATION OF ARENES

Having established an efficient benchmark catalyst for the hydrogenation of olefins, we then turned our attention to the hydrogenation reaction of more challenging substrates, i.e. substituted arenes. We started our investigation from the hydrogenation reaction of styrene (**5**) under 1 bar H<sub>2</sub> and room temperature using both Rh@D400H<sup>+</sup> and Rh@D400Li<sup>+</sup>*in* species. The time evolution of the reaction products detected in the two instances is shown in graphical format in Fig. 6. In agreement with findings discussed in the previous section, the partial hydrogenation of **5** to give ethylbenzene (**5a**) was 3.5-fold faster for Rh@D400H<sup>+</sup> (100% conversion after 40 minutes), compared to Rh@D400Li<sup>+</sup>*in* (2 hours, including the usual induction period). In both cases, the hydrogenation of the aromatic ring commenced after almost complete substrate consumption, what allowed to obtain **5a** in 100% selectivity using the protonated support and in 97% in the case of the lithiated resin. Surprisingly, the subsequent conversion of ethylbenzene to ethylcyclohexane (**5b**) followed the opposite trend, that is, it was much faster for Rh@D400Li<sup>+</sup>*in* (90% yield after 380 min), rather than for Rh@D400H<sup>+</sup> (10% yield). No other partial hydrogenation products were detected under these conditions. Direct conversion of **5** to **5b** with no intermediate detection of **5a** was possible using Rh@D400Li<sup>+</sup>*in* at higher temperatures.

The different behaviour exhibited by Rh@DLi<sup>+</sup> and Rh@DH<sup>+</sup> catalysts in olefins *versus* aromatic bonds hydrogenation is very difficult to justify. Extreme care should be taken when comparing the role of the support in MNP-based heterogeneous catalysts since a variety of additional factors may affect the



**Fig. 6** Catalytic hydrogenation reaction of **5** by Rh@D400H<sup>+</sup> (top) and Rh@D400Li<sup>+</sup>*in* (bottom). Reaction conditions: substrate 0.16 M in CH<sub>3</sub>OH, 50 mg catalyst 1.3 % (w/w) Rh, substrate / catalyst molar ratio 230, rt, H<sub>2</sub> 1 bar. Data from GC analysis.

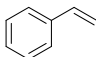
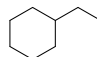
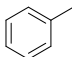
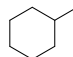
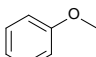
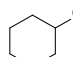
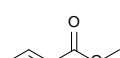
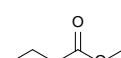
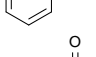
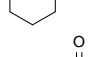
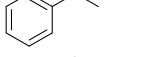
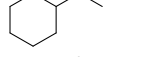
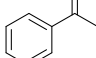
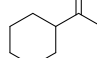
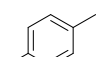
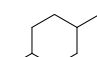
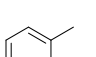
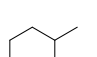
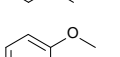
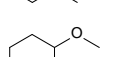
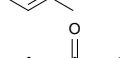
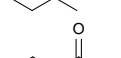


**Fig. 7** Catalytic hydrogenation reaction of **6** by Rh@D400Li<sup>+</sup>*in* and Rh@D400H<sup>+</sup>. Reaction conditions: substrate 0.16 M in CH<sub>3</sub>OH, 50 mg catalyst 1.3 % (w/w) Rh, substrate / catalyst molar ratio 230, rt, H<sub>2</sub> 1 bar. Data from GC analysis.

hydrogenation activity, including the synthetic procedure, consequently size, shape and distribution of embedded MNP,<sup>1c,59</sup> the metal-support interactions,<sup>60</sup> the mechanism of hydrogen transfer.<sup>61</sup> The latter, when involving a ionic hydrogen transfer mechanisms, may result in an activity enhancement for the protonated form of the catalyst. In our case, the diverse preparation methods required for supported MNP prevents us from a full understanding of our observations. Various models have been proposed to rationalise the role of acidic support in the catalytic activity of arene hydrogenations.<sup>62</sup> In the case of the protonated resin, we may speculate that the aromatic molecules are adsorbed on the acid sites in the form of incipient arenium ions,<sup>63</sup> that would reduce the strength of substrate chemisorption onto the rhodium surface, resulting in a low hydrogenation activity. An analogous “deactivation” effect of aromatic substrates by Brønsted acidic



**Table 4** Selected data for the catalytic hydrogenation reactions of arenes by Rh@D400Li<sup>+</sup>in.<sup>a</sup>

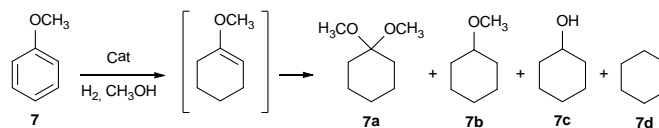
Substrate	Product	<i>T</i> (°C)	<i>P</i> H <sub>2</sub> (bar)	Time (min)	Conversion (%)	Selectivity <sup>b</sup> (%)	<i>cis</i> / <i>trans</i> ratio	TOF <sup>c</sup> (h <sup>-1</sup> )
	 <b>5b</b>	rt	1	380	99.8	89.9	-	36
	 <b>6a</b>	rt	1	345	95.0	100.0	-	38
	 <b>7b</b>	rt	10	240	98.0	63.7	-	56
		60	15	240	100.0	71.7	-	58
	 <b>8a</b>	rt	10	240	73.8	97.2	-	- <sup>d</sup>
		60	10	240	100.0	100.0	-	58
	 <b>9a</b>	rt	10	240	99.3	7.2	-	57
	 <b>10a</b>	rt	10	240	7.5	17.3	-	- <sup>d</sup>
	 <b>11a</b>	rt	10	240	100.0	100.0	76:24	58
	 <b>12a</b>	rt	10	240	63.2	100.0	94:6	- <sup>d</sup>
		60	15	240	100.0	100.0	92:8	58
	 <b>13a</b>	40	15	240	100.0	70.9	97:3	58
	 <b>14a</b>	rt	10	240	31.7	85.2	100	- <sup>d</sup>
	 <b>15a</b>	60	40	4320	76.2	37.1	91:9	- <sup>d</sup>

<sup>a</sup> Reaction conditions: 0.16 M methanol solution, substrate : metal = 230 : 1 molar ratio, 50 mg catalyst, 1.3% (w/w) Rh. Data from GC analysis. <sup>b</sup> Selectivity at the given conversion, as: (mol product indicated) / (mol substrate converted). <sup>c</sup> Turnover frequency, as: (mol substrate converted) / (mol Rh × h) calculated at the conversion indicated and bulk Rh content. <sup>d</sup> Not calculated.

supports was previously reported for the hydrogenation of styrene by RhNP onto either H<sup>+</sup> or Na<sup>+</sup>-exchanged mesoporous aluminosilicates.<sup>64</sup> A similar behaviour was described for the hydrodechlorination reaction of 1,2,4-trichlorobenzene by PdNP onto alkali-modified hydrotalcite.<sup>65</sup>

Assuming that Rh@D400Li<sup>+</sup>in is the most efficient of the prepared catalyst in the hydrogenation of arenes, we then extended our study to the hydrogenation reaction of other substituted monocyclic arenes. Selected data obtained under mild reaction conditions are summarized in Table 4, wherein selectivity to the indicated products and TOF values calculated at ≥ 95% conversions are reported for comparative purposes. Rh leaching in solution was below the ICP-OES detection limit in any case.

The reaction profile for the hydrogenation of toluene (**6**) was similar to that above described for **5** (Fig. 7). Selective conversion

**Scheme 3** Products of catalytic hydrogenation reaction of **7** by Rh@D400Li<sup>+</sup>in.

to methylcyclohexane (**6b**) was fully achieved with comparable efficiency (TOF 38 h<sup>-1</sup>) under 1 bar H<sub>2</sub> and room temperature, whereas the Rh@D400H<sup>+</sup> catalyst was much less effective. Toluene hydrogenation by solid supported-Rh(0) catalysts was previously described with various materials, including carbon nanotubes,<sup>66</sup> alumina<sup>67</sup> and silica.<sup>68</sup> The catalytic activity of Rh@D400Li<sup>+</sup>in well compares with the reported systems, while adding the advantages of easy recover and reuse. Best TOF

values were reported for 5% RhNP onto MgO (solvent-free, 100 °C, 10 bar H<sub>2</sub>)<sup>38</sup> and for tetrahedral RhNPs onto charcoal (in methanol, rt, 1 bar H<sub>2</sub>), the latter after a troublesome shape-controlled synthesis, however.<sup>69</sup>

The hydrogenation of anisole (**7**) was investigated under 10 bar H<sub>2</sub> and room temperature showing good activity, but modest selectivity to the desired hydrogenation product cyclohexyl methyl ether (**7b**, Scheme 3), since variable amounts of the hydrogenolysis products **7c**, **7d** and the acetal **7a**, that is formed by the acid-catalysed addition of methanol to the partial hydrogenation product 1-methoxy-cyclohexene (not detected), were observed, as already reported for other rhodium(0)-based catalysts.<sup>70</sup> Residual acid catalytic activity of Rh@D400Li<sup>+</sup>*in* could be attributed to spurious Brønsted acidity or to the intrinsic Lewis acidity of the rhodium metal sites.<sup>71</sup> Selectivity could be improved by the adoption of slight overhydrogenation conditions (60 °C, 15 bar) to give **7b** in 72% yield.

The hydrogenation of substrates bearing electron-withdrawing substituents (EWG) was also examined using methyl benzoate (**8**), acetophenone (**9**) and benzophenone (**10**). The reaction of **8** under 10 bar H<sub>2</sub> and room temperature resulted in incomplete substrate conversion (74%) and traces (1.5%) of the partial hydrogenation product methyl-1,2,3,6-tetrahydrobenzoate. Full conversion with 100% selectivity to methyl-cyclohexanecarboxylate (**8a**) required 60 °C and 10 bar H<sub>2</sub>. Similarly, the hydrogenation of **9** under 10 bar H<sub>2</sub> and room temperature resulted in incomplete aromatic ring hydrogenation, with concurrent preferential formation of deoxygenation and C=O bond reduction by-products, to give 2-cyclohexylethanone (**9a**) in 7.2% selectivity at 99% substrate conversion. Ring deactivation effect and scarce resistance of ketonic group toward reduction was confirmed by the hydrogenation of **10** which provided cyclohexyl(phenyl)methanone (**10a**) in 1.3% yield under the above conditions. Similar performances were previously reported in the hydrogenation of **8**, **9** and **10** using other solid-supported and colloidal RhNP catalysts under comparable, or more drastic, reaction conditions.<sup>2b</sup> Particularly, in a recent study the low chemoselectivity observed in acetophenone hydrogenation was justified by the fact that interaction of the substrate with rhodium occurs *via* the aromatic ring, so that proximity of the carbonyl group results in the reduction of the two groups at comparable rates.<sup>72</sup>

The rate of aromatic hydrogenation at Rh surface in monosubstituted arenes was previously related to both steric and electronic factors. While reduction is usually comparatively slower for longer alkyl substituents,<sup>73</sup> effect of EWG and electron-donating groups (EDG) is less certain.<sup>74</sup> It has been proposed that the hydrogenation is faster for EDG substituents because of the better adsorption of electron-rich substrates on the metal surface.<sup>75</sup> On the other hand, low rates observed for EDG groups have been attributed to the higher energy barrier toward hydrogenation due to  $\pi$ -complexation of the aromatic ring.<sup>76</sup> Substantially both hypotheses could explain our data since, despite pointing out to a EWG-deceleration effect, we

have also seen contradictory results, e.g. in the hydrogenation of **7** vs. **8**.

In order to ascertain the stereoselectivity of the Rh@D400Li<sup>+</sup>*in* catalyst, the hydrogenation of disubstituted arenes was finally tested. Whatever the substrate, the preferential formation of the kinetically favoured *cis* isomer was observed over the thermodynamically favoured *trans* one (Table 4), as usually reported for comparable heterogeneous systems, wherein the *cis/trans* ratio is affected by the nature and the position of the substituents and by the reaction temperature.<sup>77</sup> Thus, the hydrogenation of *para*- (**11**) and *ortho*-xylene (**12**) gave the dimethyl-cyclohexane derivatives **11a** and **12a** in a *cis/trans* ratio of 76:24 and 92:8 at full substrate conversion, respectively, though slightly harder reaction conditions were required to achieve comparable reaction rate in the latter case (60 °C and 15 bar vs. rt and 10 bar). Similar results were previously reported for RhNP onto boehmite nanofibers<sup>78</sup> or Rh@MWCNT,<sup>24</sup> and justified in terms of limited Rh-sites accessibility of C=C bonds due to the larger steric hindrance of **12**. Compared to the hydrogenation reaction of the parent monosubstituted arene, i.e. toluene (**6**), both **11** and **12** showed to be hydrogenated with much less efficiency under the same reaction conditions (rt and 1 bar, TOF = 20 h<sup>-1</sup> and 3 h<sup>-1</sup>, respectively), as commonly found with increasing the number of substituents.<sup>2b</sup>

The hydrogenation reaction of 2-methylanisole (**13**) was in line with the selectivity results above described for **7**. Hence, the desired aromatic hydrogenation product 1-methoxy-2-methylcyclohexane (**13a**) was obtained in 71% yield at 100% substrate conversion under 40 °C and 1 bar H<sub>2</sub>, with a *cis/trans* ratio of 97:3. By-products due to acetalization and hydrogenolysis were observed. A similar performance was previously reported for rhodium colloids impregnated onto silica which afforded **13a** in a 98:2 *cis/trans* ratio.<sup>79</sup> The hydrogenation of methyl-2-methylbenzoate (**14**) was possible under room temperature and 10 bar, although with slow kinetic, to give selectively methyl-2-methylcyclohexanecarboxylate (**14a**) as single *cis* isomer, together with minor amounts of dihydrogenated products. The hydrogenation of methyl-2-aminobenzoate (**15**) was very slow, as 76.2% conversion was achieved after 72h, resulting in the formation of **15a** with a *cis/trans* ratio of 91:9 and considerable amount of dihydrogenated products. Deactivation of **15** was previously attributed to strong substrate adsorption on the metal surface through the amino group.<sup>80</sup> An 80% yield with a *cis/trans* ratio of 6 after 210 h reaction time was reported using Ru colloids. To the best of our knowledge no supported rhodium catalysts have been reported for the hydrogenation reaction of **14** and **15**.

## Conclusions

On the route to a sustainable nanocatalysis, we have developed a friendly and reproducible method for the growth of RhNP within the pores of commercially available insoluble polymers. The synthetic procedure involves the atomic-level distribution of an appropriate Rh precursor within the solid matrix by

impregnation,<sup>81</sup> followed by reduction using clean reducing agents (H<sub>2</sub>), low energy inputs (rt, 1 bar) and without stabilizers or long conditioning steps, thus accomplishing with most Principles of Greener Nanomaterial Production.<sup>82</sup> The as-prepared supported RhNP have shown to efficiently catalyse the hydrogenation reaction of C=C bonds under very undemanding conditions, as well as to be easily recovered with neither activity loss nor metal leaching in solution upon reuse. Following the same paradigm pursued for the corresponding palladium systems, we have explored the effect of both the preparation method and the ionic form of the support on the catalyst performance. It has been shown that, while the hydrogenation of alkenes is best achieved using the supported catalyst in the protonated form, the hydrogenation of aromatics is much more favourably accomplished using the lithiated catalyst prepared *in-situ* under catalytic conditions. The latter system allows for the heterogeneous-phase hydrogenation of mono- and di-substituted arenes to take place in one-pot at temperatures below 60 °C and H<sub>2</sub> pressures below 15 bar, thus representing a sustainable option for this reaction.

### Acknowledgements

Thanks are due to Centro Microscopia Elettronica - Area di Ricerca CNR, Firenze for technical support.

### Notes and references

- For recent reviews on RhNP catalysts, see: (a) N. Yan, Y. Yuan and P. J. Dyson, *Dalton Trans.* 2013, **42**, 13294 - 13304; (b) L. M. Rossi, L. L. R. Vono, M. A. S. Garcia, T. L. T. Faria and J. A. Lopez-Sanchez, *Top. Catal.* 2013, **56**, 1228 - 1238; (c) Y. Yuan, N. Yan and P. J. Dyson, *ACS Catal.* 2012, **2**, 1057 - 1069; (d) A. Roucoux, A. Nowicki and K. Philippot in *Nanoparticle and Catalysis*, Ed. D. Astruc, Wiley-VCH, Weinheim, 2007, ch. 11, pp. 349 - 388.
- For recent reviews on the catalytic hydrogenation reaction of arenes, see: (a) M. Guerrero, N. T. Than Chau, S. Noel, A. Denicourt-Nowicki, F. Hapiot, A. Roucoux, E. Monflier and K. Philippot, *Curr. Org. Chem.* 2013, **17**, 364 - 399; (b) A. Gual, C. Godard, S. Castillón and C. Claver, *Dalton Trans.* 2010, **39**, 11499 - 11512.
- B. Pugin and H. U. Blaser, *Top. Catal.* 2010, **53**, 953.
- N. End and K. U. Schöning in *Immobilized Catalysts: Solid Phases, Immobilization and Applications*, Ed. A. Kirschning, Springer, Heidelberg, 2004, pp. 241 - 272.
- CRC Handbook of Chemistry and Physics*; Ed. W. M. Haynes., CRC Press: Boca Raton, 2013, 94th edition, Section 4.
- Kitco Metals Inc., [www.kitco.com/charts/rhodium.html](http://www.kitco.com/charts/rhodium.html).
- (a) C. A. Witham, W. Huang, C. K. Tsung, J. N. Kuhn, G. A. Somorjai and F. D. Toste, *Nat. Chem.*, 2010, **2**, 36 - 41; (b) A. Fukuoka and P. L. Dhepe, *Chem. Rec.* 2009, **9**, 224 - 235; (c) N. Semagina and L. Kiwi-Minsker, *Catal. Rev. Sci. Eng.* 2009, **51**, 147 - 217.
- J. M. Campelo, D. Luna, R. Luque, J. M. Marinas and A. A. Romero, *ChemSusChem*, 2009, **2**, 18 - 45.
- (a) S. Sarkar, E. Guibal, F. Quignard and A. K. SenGupta, *J. Nanopart. Res.* 2012, **14**, 715 - 739; (b) P. Barbaro and F. Liguori, *Chem. Rev.* 2009, **109**, 515 - 529; (c) G. Gelbard, *Ind. Eng. Chem. Res.* 2005, **44**, 8468 - 8498.
- A. A. Zagorodni, *Ion Exchange Materials: Properties and Applications*, Elsevier, Amsterdam, 2006.
- A. Roucoux, J. Schulz and H. Patin, *Chem. Rev.* 2002, **102**, 3757 - 3778.
- (a) B. Corain, K. Jeřábek, P. Centomo and P. Canton, *Angew. Chem., Int. Ed.* 2004, **43**, 959 - 962; (b) H. Bönemann and R. M. Richards, *Eur. J. Inorg. Chem.* 2001, 2455 - 2480.
- B. Corain, M. Zecca and K. Jeřábek, *J. Mol. Catal.* 2001, **177**, 3 - 20.
- (a) B. Corain, M. Zecca, P. Canton and P. Centomo, *Phil. Trans. R. Soc. A* 2010, **368**, 1495 - 1507; (b) M. Zecca, P. Centomo and B. Corain in *Metal Nanoclusters in Catalysis and Materials Science*, Eds. B. Corain, G. Schmid and N. Toshima, Elsevier, Amsterdam, 2008, pp. 201 - 232.
- (a) T. Seki, J. D. Grunwaldt, N. van Vegten and A. Baiker, *Adv. Synth. Catal.* 2008, **350**, 691 - 705; (b) W. Laufer, J. P. M. Niederer and W. F. Hoelderich, *Adv. Synth. Catal.* 2002, **34**, 1084 - 1089.
- C. Moreno Marrofan, D. Berti, F. Liguori and P. Barbaro, *Catal. Sci. Technol.* 2012, **2**, 2279 - 2290.
- F. Liguori and P. Barbaro, *J. Catal.* 2014, **311**, 212 - 220.
- Pd(NO<sub>3</sub>)<sub>2</sub> or [Pd(CH<sub>3</sub>CN)<sub>4</sub>](BF<sub>4</sub>)<sub>2</sub> in the case of palladium.
- P. Barbaro, C. Bianchini, G. Giambastiani, W. Oberhauser, L. Morassi Bonzi, F. Rossi and V. Dal Santo, *J. Chem. Soc., Dalton Trans.* 2004, 1783 - 1784.
- (a) M. A. Esteruelas and L. A. Oro, *Chem. Rev.* 1998, **98**, 577 - 588; (b) R. R. Schrock and J. A. Osborn, *J. Am. Chem. Soc.* 1971, **93**, 3089 - 3091; (c) R. R. Schrock and J. A. Osborn, *J. Am. Chem. Soc.* 1971, **93**, 2397 - 2407.
- A. J. Bard, R. Parsons, J. Jordan, *Standard potential in aqueous solution*, Dekker, New York, 1985.
- (a) S. Agarwal and J. N. Ganguli, *J. Mol. Catal. A: Chem.* 2013, **372**, 44 - 50; (b) K.B. Sidhpuria, H.A. P. Patel, A. Parikh, P. Bahadur, H.C. Bajaj and R.V. Jasra, *Appl. Clay Sci.* 2009, **42**, 386 - 390; (c) H.A. Patel, H.C. Bajaj and R.V. Jasra, *J. Nanopart. Res.* 2008, **10**, 625 - 632; (d) Sz. Papp, A. Oszko and I. Dékány, *Chem. Mater.* 2004, **16**, 1674 - 1685.
- (a) S. Niembro, S. Donnici, A. Shafir, A.a Vallribera, M. L. Buil, M. A. Esteruelas and C. Larramona, *New J. Chem.* 2013, **37**, 278 - 282; (b) M. Boutros, G. Shirley, T. Onfroy and F. Launay, *Appl. Catal., A* 2011, **394**, 158 - 165.
- H. B. Pan, C. M. Wai, *J. Phys. Chem. C* 2010, **114**, 11364 - 11369.
- (a) R. B. Duarte, F. Krumeich and J. A. van Bokhoven, *ACS Catal.* 2014, **4**, 1279 - 1286; (b) R. B. Duarte, M. Nachtegaal, J. M. C. Bueno and van J. A. Bokhoven, *J. Catal.* 2012, **296**, 86 - 98.
- M. H. Halabi, M. H. J. M de Croon, J. van der Schaaf, P. D. Cobden and J. C. Schouten, *Appl. Catal., A* 2010, **389**, 68 - 79.
- D. A. J. M. Ligthart, R. A. van Santen and E. J. M. Hensen, *J. Catal.* 2011, **280**, 206 - 220.

- 28 D. Mei, V. A. Glezakou, V. Lebarbier, L. Kovarik, H. Wan, K. O. Albrecht, M. Gerber, R. Rousseau and R. A. Dagle, *J. Catal.* 2014, **316**, 11 - 23.
- 29 D. F. Han, X. H. Li, H. D. Zhang, Z. M. Liu, J. Li, C. Li, *J. Catal.* 2006, **243**, 318 - 328.
- 30 M. E. Grass, S. H. Joo, Y. Zhang and G. A. Somorjai, *J. Phys. Chem. C* 2009, **113**, 8616 - 8623.
- 31 A. Siani, O. S. Alexeev, D. S. Deutsch, J. R. Monnier, P. T. Fanson, H. Hirata, S. Matsumoto, C. T. Williams and M. D. Amiridis, *J. Catal.* 2009, **266**, 331 - 342.
- 32 (a) M. L. Buil, M. A. Esteruelas, S. Niembro, M. Oliván, L. Orzechowski, C. Pelayo and A. Vallribera, *Organometallics* 2010, **29**, 4375 - 4383; (b) V. K. Kanuru, S. M. Humphrey, J. M. W. Kyffin, D. A. Jefferson, J. W. Burton, M. Armbruster and R. M. Lambert, *Dalton Trans.* 2009, 7602 - 7605; (c) M. Ojeda, S. Rojas, M. Boutonnet, F. J. Perez-Alonso, F. J. Garcia-García and J. L. G. Fierro, *Appl. Catal.*, A 2004, **274**, 33 - 41.
- 33 C. Hubert, A. Denicourt-Nowicki, P. Beaunier and A. Roucoux, *Green Chem.* 2010, **12**, 1167 - 1170.
- 34 S. M. McClure, M. J. Lundwall and D. W. Goodman, *Proc. Natl. Acad. Sci. U.S.A.* 2011, **108**, 931 - 936.
- 35 F. Hoxha, N. van Vegten, A. Urakawa, F. Krumeich, T. Mallat and A. Baiker, *J. Catal.* 2009, **261**, 224 - 231.
- 36 N. Savastenko, H. R. Volpp, O. Gerlach and W. Strehlau, *J. Nanopart. Res.* 2008, **10**, 277 - 287.
- 37 One-pot generation of RhNP onto aluminum oxyhydroxide at 373 K was also reported, see: I. S. Park, M. S. Kwon, K. Y. Kang, J. S. Lee and J. Park, *Adv. Synth. Catal.* 2007, **349**, 2039 - 2047.
- 38 A. Sánchez, M. Fang, A. Ahmed and R. A. Sánchez-Delgado, *Appl. Catal. A: General* 2014, **477**, 117 - 124
- 39 An outer shell of depth ca. 2  $\mu\text{m}$  having a mean Rh loading of ca. 2.7 % (w/w) and an inner mean Rh loading of ca. 0.8 % (w/w) were estimated from EDS analyses carried out on sections of Rh@D100Li<sup>+</sup> reduced beads, that well matches the bulk Rh content value obtained from ICP-OES measurement.
- 40 (a) F. Liguori, C. Moreno-Marrodan and P. Barbaro, *Chinese J. Catal.* 2015, DOI: 10.1016/S1872-2067(15)60865-8; (b) C. Moreno-Marrodan and P. Barbaro, *Green Chem.* 2014, **16**, 3434 - 3438; (c) L. Calore, G. Cavinato, P. Canton, L. Peruzzo, R. Banavali, K. Jeřábek and B. Corain, *Inorg. Chim. Acta* 2012, **391**, 114 - 120.
- 41 M. Králík, M. Hronec, S. Lora, G. Palma, M. Zecca, A. Biffis and B. Corain, *J. Mol. Catal. A: Chem.* 1995, **97**, 145 - 155.
- 42 A. Biffis, H. Landes, K. Jeřábek and B. Corain, *J. Mol. Catal. A: Chemical* 2000, **151**, 283 - 288.
- 43 A surface/bulk metal atoms ratio of ca. 18% was estimated from TEM data, see: R. L. Johnston, *Atomic and Molecular Clusters*, Taylor & Francis, London, 2002.
- 44 F. Liguori and P. Barbaro, *Catal. Sci. Technol.* 2014, **4**, 3835 - 3839.
- 45 C. Moreno-Marrodan, P. Barbaro, M. Catalano and A. Taurino, *Dalton Trans.* 2012, **41**, 12666 - 12669.
- 46 L. Huang, P. Luo, W. Pei, X. Liu, Y. Wang, J. Wang, W. Xing and J. Huang, *Adv. Synth. Catal.* 2012, **354**, 2689 - 2694.
- 47 M. J. Jacinto, P. K. Kiyohara, S. H. Masunaga, R. F. Jardim and L. M. Rossi, *Appl. Catal. A* 2008, **338**, 52 - 57
- 48 (a) J. Toubiana, M. Chidambaram, A. Santo and Y. Sasson, *Adv. Synth. Catal.* 2008, **350**, 1230 - 1234; (b) N. Kim, M. S. Kwon, C. M. Park and J. Park, *Tetrahedron Lett.* 2004, **45**, 7057 - 7059.
- 49 Maitlis catalyst leaching test, see: J. P. Collman, K. M. Kosydar, M. Bressan, W. Lamanna and T. Garrett, *J. Am. Chem. Soc.* 1984, **106**, 2569 - 2579.
- 50 T. Seki, J. D. Grunwaldt and A. Baiker, *Chem. Commun.* 2007, 3562 - 3564
- 51 A. Drelinkiewicz, A. Knapik, A. Waksmundzka-Góra, A. Bukowska, W. Bukowski and J. Noworól, *React. Funct. Polym.* 2008, **68**, 1059 - 1071.
- 52 C. Perego and S. Peratello, *Catal. Today* 1999, **52**, 133 - 145.
- 53 TEM data indicated that the size of embedded RhNP is not significantly affected from the size of the resin beads.
- 54 T. Miller, B. L. Mojet, D. E. Ramaker and D. C. Koningsberger, *Catal. Today* 2000, **62**, 101 - 114.
- 55 A. M. R. Galletti, C. Antonetti, V. De Luise and M. Martinelli, *Green Chem.* 2012, **14**, 688 - 694.
- 56 R. Selke, K. Häupke and W. Krause, *J. Mol. Catal.* 1989, **56**, 315 - 328.
- 57 See Supplementary Information for experimental results tables.
- 58 Induction period were observed in some instance for PdNP hydrogenation catalysts, see: (a) P. Centomo, M. Zecca, M. Kralik, D. Gasparovicova, K. Jeřábek, P. Canton and B. Corain, *J. Mol. Catal. A: Chem.* 2009, **300**, 48 - 58; (b) L. Durán Pachón, C. J. Elsevier and G. Rothenberg, *Adv. Synth. Catal.* 2006, **348**, 1705 - 1710.
- 59 B. Corain and M. Kralik, *J. Mol. Catal. A: Chem.* 2000, **159**, 153 - 162.
- 60 W. P. Zhou, A. Lewera, R. Larsen, R. I. Masel, P. S. Bagus and A. Wieckowski, *J. Phys. Chem. B* 2006, **110**, 13393 - 13398.
- 61 J. Wang, L. M. Huang and Q. Z. Li, *Appl. Catal. A* 1998, **175**, 191 - 199.
- 62 (a) A. Stanislaus and B. H. Cooper, *Catal. Rev. Sci. Eng.* 1994, **36**, 75 - 123; (b) S. D. Lin and M. A. Vannice, *J. Catal.* 1993, **143**, 563 - 572.
- 63 (a) E. Garbowski and M. Primet, *J. Chem. Soc., Faraday Trans. 1* 1987, **83**, 1469 - 1476; (b) D. H. Olson and W. O. Haag, *Am. Chem. Soc. Symp. Ser.* 1984, **248**, 275 - 286.
- 64 M. Boutros, A. Denicourt-Nowicki, A. Roucoux, L. Gengembre, P. Beaunier, A. Gédéon and F. Launay, *Chem. Commun.* 2008, 2920 - 2922.
- 65 B.T. Meshesha, R.J. Chimentao, A.M. Segarra, J. Llorca, F. Medina, B. Coq and J. E. Sueiras, *Appl. Catal. B: Env.* 2011, **105** 361 - 372.
- 66 B. Yoon, H. B. Pan and Chien M. Wai, *J. Phys. Chem. C* 2009, **113**, 1520 - 1525.
- 67 N. A. Dehm, X. Zhang and J. M. Buriak, *Inorg. Chem.* 2010, **49**, 2706 - 2714.
- 68 K. J. Stanger, Y. Tang, J. Anderegg and R. J. Angelici, *J. Mol. Catal. A: Chem.* 2003, **202**, 147 - 161.

- 69 K. H. Park, K. Jang, H. J. Kim and S. U. Son, *Angew. Chem. Int. Ed.* 2007, **46**, 1152 – 1155.
- 70 (a) C. Hubert, A. Denicourt-Nowicki, J. Guegan and A. Roucoux, *Dalton Trans.* 2009, 7356 – 7358; (b) J. A. Widegren and R. G. Finke, *Inorg. Chem.* 2002, **41**, 1558 – 1572.
- 71 N. Scotti, M. Dangate, A. Gervasini, C. Evangelisti, N. Ravasio and F. Zaccheria, *ACS Catal.* 2014, **4**, 2818 – 2826.
- 72 J. L. Castelbou, E. Bres-Femenia, P. Blondeau, B. Chaudret, S. Castellón, C. Claver and C. Godard, *ChemCatChem* 2014, **6**, 3160 – 3168.
- 73 S. Toppinen, T. K. Rantakyla, T. Salmi and J. Aittamaa, *Ind. Eng. Chem. Res.* 1996, **35**, 4424-4433.
- 74 F. Lu, J. Liu and J. Xu, *J. Mol. Catal. A: Chem.* 2007, **271**, 6 - 13.
- 75 J. Schulz, A. Roucoux and H. Patin, *Chem. Eur. J.* 2000, **6**, 618-624.
- 76 M. Zahmakıran, Y. Román-Leshkov and Y. Zhang, *Langmuir*, 2012, **28**, 60 – 64.
- 77 J. A. Widegren, R. G. Finke, *J. Mol. Catal. A: Chem.* 2003, **191**, 187 - 207.
- 78 I. S. Park, M. S. Kwon, N. Kim, J. S. Lee, K. Y. Kang and J. Park, *Chem. Commun.*, 2005, 5667 – 5669.
- 79 V. Mévellec, A. Nowicki, A. Roucoux, C. Dujardin, P. Granger, E. Payen and K. Philippot, *New J. Chem.* 2006, **30**, 1214 – 1219.
- 80 F. Fache, S. Lehuède and M. Lemaire, *Tetrahedron Lett.* 1995, **36**, 885-888.
- 81 B. Corain and M. Králik, *J. Mol. Catal. A: Chem.* 2001, **173**, 99 – 115.
- 82 J. A. Dahl, B. L. S. Maddux and J. E. Hutchison, *Chem. Rev.* 2007, **107**, 2228 – 2269.